Mathematical Biosciences and Engineering

MBE, 16(5): 6034–6046.
DOI: 10.3934/mbe.2019302
Received: 26 March 2019
Accepted: 13 June 2019
Published: 29 June 2019

http://www.aimspress.com/journal/MBE

Research article

Wavelet filtering of fetal phonocardiography: A comparative analysis

Selene Tomassini [1], Annachiara Strazza [2], Agnese Sbrollini [1], Ilaria Marcantoni [1], Micaela Morettini [1], Sandro Fioretti [2] and Laura Burattini [1,2,*]

[1] Cardiovascular Bioengineering Lab, Department of Information Engineering, Universit à Politecnica delle Marche, Ancona, Italy
[2] Laboratorio di Bioingegneria, Department of Information Engineering, Universit à Politecnica delle Marche, Ancona, Italy

*** Correspondence:** Email: l.burattini@univpm.it; Tel: +39 071 220 4461; Fax: +39 071 220 4224.

Abstract: Fetal heart rate (FHR) monitoring can serve as a benchmark to identify high-risk fetuses. Fetal phonocardiogram (FPCG) is the recording of the fetal heart sounds (FHS) by means of a small acoustic sensor placed on maternal abdomen. Being heavily contaminated by noise, FPCG processing implies mandatory filtering to make FPCG clinically usable. Aim of the present study was to perform a comparative analysis of filters based on Wavelet transform (WT) characterized by different combinations of mothers Wavelet and thresholding settings. By combining three mothers Wavelet (4^{th}-order Coiflet, 4^{th}-order Daubechies and 8^{th}-order Symlet), two thresholding rules (Soft and Hard) and three thresholding algorithms (Universal, Rigorous and Minimax), 18 different WT-based filters were obtained and applied to 37 simulated and 119 experimental FPCG data (PhysioNet/PhysioBank). Filters performance was evaluated in terms of reliability in FHR estimation from filtered FPCG and noise reduction quantified by the signal-to-noise ratio (SNR). The filter obtained by combining the 4^{th}-order Coiflet mother Wavelet with the Soft thresholding rule and the Universal thresholding algorithm was found to be optimal in both simulated and experimental FPCG data, since able to maintain FHR with respect to reference (138.7[137.7; 140.8] bpm vs. 140.2[139.7; 140.7] bpm, $P > 0.05$, in simulated FPCG data; 139.6[113.4; 144.2] bpm vs. 140.5[135.2; 146.3] bpm, $P > 0.05$, in experimental FPCG data) while strongly incrementing SNR (25.9[20.4; 31.3] dB vs. 0.7[−0.2; 2.9] dB, $P < 10^{-14}$, in simulated FPCG data; 22.9[20.1; 25.7] dB vs. 15.6[13.8; 16.7] dB, $P < 10^{-37}$, in experimental FPCG data). In conclusion, the WT-based filter obtained combining the 4^{th}-order Coiflet mother Wavelet with the thresholding settings constituted by the Soft rule and the Universal algorithm provides the optimal WT-based filter for FPCG filtering according to evaluation criteria based on both noise and clinical features.

Keywords: fetal monitoring; fetal phonocardiography; mothers wavelet; thresholding settings; wavelet transform filtering

Abbreviations

FHR: Fetal Heart Rate; FHS: Fetal Heart Sounds; FPCG: Fetal PhonoCardioGram; SNR: Signal-to-Noise Ratio; WT: Wavelet Transform

1. Introduction

Fetal monitoring, often consisting in the monitoring of the fetal cardiac activity, is finalized to understand the normal autonomic maturation of the fetus and can serve as a benchmark to identify high-risk fetuses. Fetal heart rate (FHR) is one of the most commonly monitored features due to the important clinical information that can be derived from its analysis. Normal FHR values range from 110 bpm to 160 bpm. Prolonged (lasting more than 10 min) FHR deviations from this range indicate abnormal and possibly pathological fetal conditions [1]. Fetal tachycardia is usually due to maternal pyrexia, epidural analgesia, and sometimes, catecholamine secretion during the initial stages of a non-acute fetal hypoxemia. Instead, bradycardia is mainly due to maternal hypothermia, maternal use of beta-blocker drugs and fetal arrhythmias, even though it can also occur in normal fetuses of postdate pregnancies. Short (lasting at most 15 s) FHR deviations are also clinically relevant. If accelerations mainly indicate a neurologically responsive fetus, decelerations often indicate a critical health status. Thus, a correct identification of FHR is fundamental in the prenatal clinical investigations [1–9].

Fetal phonocardiography consists in the recording of the fetal heart sounds (FHS) by means of a small acoustic sensor placed on maternal abdomen (Figure 1). The acquired acoustic signal is then transduced into an electric signal, termed fetal phonocardiogram (FPCG), that can be visually or automatically analyzed [10,11]. FHS [2,12–13] are non-stationary natural vibro-acoustic waves produced by the fetal heart mechanical activity during a cardiac cycle. Specifically, they are short bursts of vibratory energy caused by cardiac valves movements with an acoustic character and a relatively short duration. There are two major sounds for each cardiac cycle. The first sound, which is the longest and loudest, corresponds to the asynchronous closure of mitral and tricuspid valves during the isovolumic contraction phase of the systole. On FPCG, the first sound is represented by the S1 waveform [3,12] that is characterized by a low frequency (20–40 Hz) spectral content. The second sound corresponds to the asynchronous closure of aortic and pulmonary valves during the isovolumic relaxation phase of the diastole; typically, it is shorter and less loud than the first sound due to anatomical differences in the valve leaflets (semilunar valves are more stretched than atrioventricular valves [14]). On FPCG, the second sound is represented by the S2 waveform [3,12] that is characterized by a high frequency (50–70 Hz) spectral content. The time interval between two consecutive S1 (or between two consecutive S2) waveforms represents the fetal cardiac period from which FHR can be derived.

Compared to other fetal monitoring techniques, mainly the popular cardiotocography [15] and the indirect fetal electrocardiography [16–19], the fetal phonocardiography [2,3,9,11,12,20–23] is more suitable for continuous and long-term fetal monitoring, which is very desirable to promptly identify and treat possible fetal complications during pregnancy. Indeed, fetal phonocardiography is

non-invasive, completely harmless (as no energy is emitted), affordable (due to its low cost), easy to manage in any environment (even domestic), user-independent and can be performed at any stage of pregnancy. Differently, cardiotocography cannot be used for long-term fetal monitoring due to its high cost and instrumentation complexity; on the other hand, non-invasive fetal electrocardiography, although measurable approximately starting from the 20th week of gestation, becomes more clinically significant and reliable during the last weeks of gestation, when the vernix caseosa layer surrounding and electrically shielding the fetus dissolves [16–19]. Despite its potential, wide spread of continuous and long-term fetal phonocardiographic monitoring is still limited by difficulties in automatic processing: FPCG is a signal heavily corrupted by noise and designing automatic procedures to denoise it remains very challenging [11,23]. Indeed, there are several sources of noise corrupting FPCG. FHS propagate from the internal acoustic source (i.e. the fetal heart) to the external acoustic receiver (i.e. the sensor) through a time-varying transmission pathway made up of several different layers (amniotic fluid, uterus muscular wall, fat tissue, etc.), each having different attenuation, reflection and refraction properties [11,23,24]. Additionally, sounds generated by physiological and non-physiological sources located nearby may interfere. Overall, noise affecting FPCG is classified as internal noise or external noise [11]. The internal noise [3,12] is a random corrupting acoustic signal mainly generated by maternal heart activity (10–40 Hz), maternal respiration, maternal digestion, placental blood turbulence and fetal movements (0–25 Hz). Instead, the external noise [4] is mainly due to power line interference (50/60 Hz), environmental noise and sensor movement during acquisition (all spectrum). As a consequence, the acquired raw FPCG results to be a superimposition of FHS, which is the signal of interest, and other sounds due to internal or external noise (Figure 1). Thus, FPCG is typically characterized by a low signal-to-noise ratio (SNR) and the frequency bands of maternal heart sounds and FHS overlap, making FPCG filtering very challenging [23].

As it is heavily contaminated by noise, FPCG processing implies mandatory filtering to make it clinically usable. Conventional approaches based on linear low-pass and high-pass filtering are not efficient [25] due to the existence of frequency bands in which FPCG and noise components overlap. Differently, filtering procedures based on Wavelet transform (WT) demonstrated to be promising [2,11,12,21,24–30]. Indeed, WT performs a correlation analysis; thus, its output is maximal when the input FPCG signal most resembles the chosen mother Wavelet. Additionally, WT decomposes data features into different scales. Since the FPCG signal has its energy concentrated in few WT levels [12,21,28–30], the few related WT coefficients are relatively large compared to the several coefficients related to noise, which is typically spread over several WT levels. WT filtering also includes a thresholding procedure to remove the low coefficients related to noise; eventually, the inverse WT is applied to get a filtered FPCG. The WT-based filters proposed in literature differ for used mothers Wavelet and thresholding settings (rules and algorithms). In particular, an interesting study by Chourasia et al. [29] compared several combinations of mothers Wavelet and thresholding settings and concluded that the 4th-order Coiflet mother Wavelet combined with Soft rule and Rigorous algorithm shows the best performance. However, evaluation has been done using only a noise-related feature (i.e. the mean squared error) and no clinical features. Consequently, clinical significance of the results has not been demonstrated since noise removal could indeed cause removal of some clinically useful FPCG components. Thus, the aim of the present work was to perform a comparative analysis of WT-based FPCG filtering approaches characterized by different combinations of mothers Wavelet and thresholding settings by considering both a noise-related feature, i.e. SNR, and the main clinical feature, i.e. FHR.

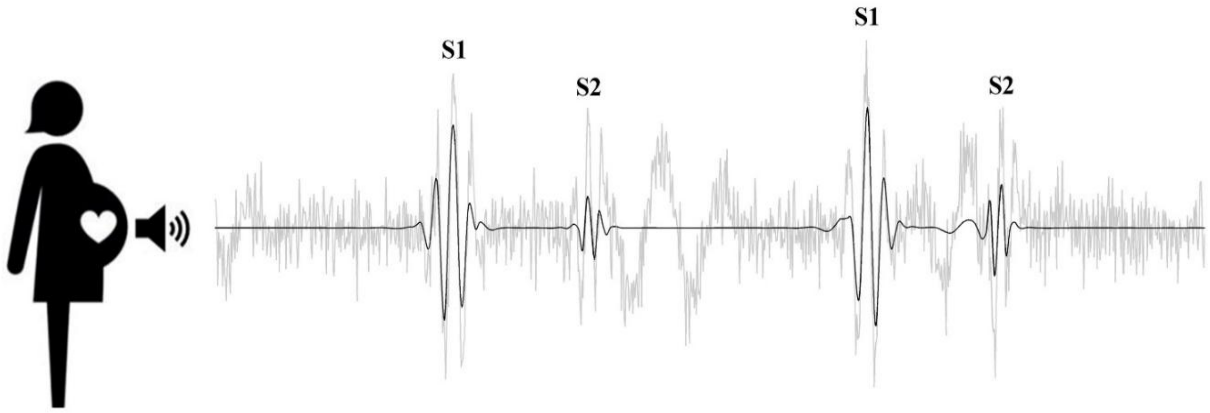

Figure 1. Raw FPCG (in gray), acquired by a small acoustic sensor placed on maternal abdomen, is heavily corrupted by noise and needs to be filtered to be clinically usable. Filtered FPCG (in black) is mainly constituted by two waveforms: S1, representing the sound generated by the asynchronous closure of mitral and tricuspid valves during the isovolumic contraction phase of the systole; and S2, representing the sound generated by the asynchronous closure of aortic and pulmonary valves during the isovolumic relaxation phase of the diastole.

2. Methods

In this study, both simulated and experimental raw FPCG (all available at PhysioNet/PhysioBank [31]) were filtered through 18 WT-based filtering approaches, each characterized by a different combination of mother Wavelet and thresholding settings. Filtered FPCG were then analyzed to evaluate FHR and noise reduction (SNR increment). The optimal WT-based filter was eventually identified as the one allowing the most accurate FHR evaluation and the highest SNR increment.

2.1. Data

2.1.1. Simulated data

Simulated FPCG data belong to the 'Simulated Fetal PCGs database' [4,32] and consist of 37 simulated FPCG obtained by summation of a sequence of simulated S1 and S2 waveforms with various kinds and levels of simulated internal and external noise. Simulated raw FPCG (sampling frequency: 1 kHz) were 8 min long. FHR values were obtained after manually annotating S1. SNR ranged from −1.11 dB to 7.37 dB. Such values of FHR and SNR were taken as reference when evaluating performances of a WT-based filter on simulated FPCG data.

2.1.2. Experimental data

Experimental FPCG data belong to the 'Shiraz University (SU) fetal heart sounds database' [22,33] and consist of 119 FPCG recorded on 109 pregnant women (99 women had one FPCG recorded, 3 had

two FPCG recorded, and 7 had FPCG of twins recorded individually). Experimental raw FPCG duration ranged from 28.65 s to 133.17 s; sampling frequency was generally 16 kHz, with a few signals recorded at 44 Hz and 100 Hz [22,33]. FHR relative to each raw FPCG was indirectly computed by using the FHR signal of simultaneously acquired cardiotocographic recordings; over the database, it ranged from 121.3 bpm to 172.1 bpm. SNR ranged from 9.6 dB to 21.6 dB. Such values of FHR and SNR were taken as reference when evaluating performances of a WT-based filtering procedures on experimental FPCG data.

2.2. Processing procedure

2.2.1. Pre-processing

Each simulated and experimental FPCG was normalized by its maximum amplitude and rescaled so that its amplitude could vary between ±100. Normalized FPCG were pre-filtered by application of a conventional band-pass filter (3^{rd}-order Butterworth filter with cut-off frequencies at 20 Hz and 120 Hz [21,28]) before being submitted to a WT-based filter for further noise removal (Figure 2).

2.2.2. Wavelet transform-based filtering procedure

The proposed WT-based filtering procedure consists of three main steps (Figure 2): WT decomposition, denoising and reconstruction. Decomposition was performed on 7 levels (which we previously found to be suitable for WT-based FPCG filtering [21,28]) by using 3 different mothers Wavelet, namely the 4^{th}-order Coiflet, the 4^{th}-order Daubechies and the 8^{th}-order Symlet, selected based on their morphological closeness to S1 and S2 waveforms [21,29,34,35] and to their orthogonality [26]. Once the pre-processed FPCG was decomposed, the levels introducing noise were removed according to predefined thresholding settings. Specifically, two thresholding rules, namely Soft and Hard, and three thresholding algorithms, namely Universal, Rigorous, and Minimax, were considered, being those the most commonly employed for non-stationary signals filtering [2,12,26,29,35]. Eventually, the filtered FPCG was obtained by WT reconstruction. All possible combinations of mothers Wavelet, thresholding rules and thresholding algorithms were considered, so that 18 different WT-based filters (F1 to F18; Table 1) were obtained.

2.3. Features extraction and statistics

Each filtered FPCG, either from simulated or experimental data, was characterized in terms of FHR, SNR and error (ε_{FHR}). Specifically, from each filtered FPCG, S1 sounds were automatically identified using PCG-Delineator, a previously published threshold-based application for accurate computerized identification of FPCG waveforms (S1 and S2) [28].

Successively, FHR (bpm) was evaluated as in Eq. 1, where fs indicates the sampling frequency and $\overline{S1S1}$ represents the mean number of samples between two consecutive S1 waveforms:

$$FHR = 60 * fs/\overline{S1S1}\,. \qquad (1)$$

SNR (dB) was calculated as in Eq. 2, where max(FPCG), min(FPCG) and std(FPCG) respectively indicate FPCG maximum, minimum and standard deviation [21]:

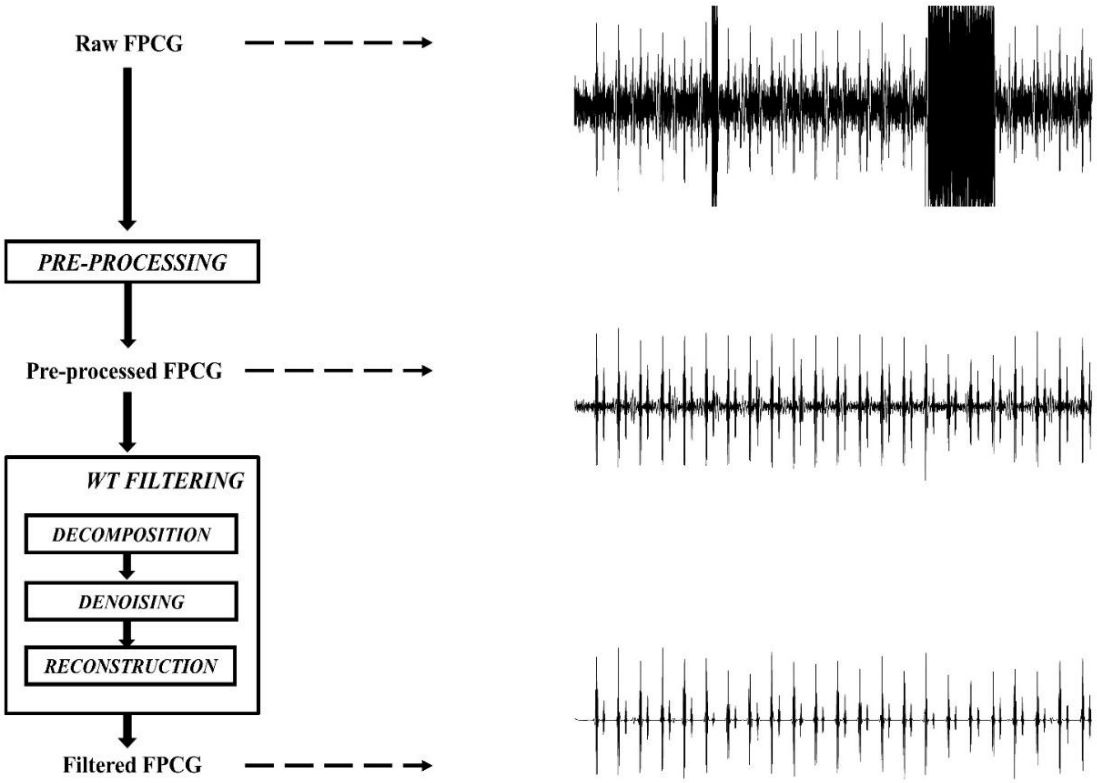

Figure 2. WT-based procedure for FPCG filtering: the raw FPCG is pre-processed before being submitted to a WT-based filter.

$$SNR = 20 * Log\left(\frac{max(FPCG)-min(FPCG)}{4*std(FPCG)}\right). \qquad (2)$$

Eventually, ε_{FHR} (bpm) was computed ad in Eq. 3, where FHR_{Ref} and FHR_{WT} are respectively the reference FHR and the FHR of the WT-filtered FPCG:

$$\varepsilon_{FHR} = FHR_{Ref} - FHR_{WT}. \qquad (3)$$

Normality of FHR and SNR distributions over simulated and experimental FPCG data were evaluated using the Lilliefors test. Non-normal distributions were described in terms of $50^{th}[25^{th};75^{th}]$ percentiles and compared by means of the Wilcoxon Rank-Sum test. Statistical level of significance (P) was set at 0.05.

2.4. Optimal filter identification

Identification of the optimal WT-based filter, that is of the optimal combination of mother

Wavelet and thresholding settings, occurred by applying the following evaluation criteria. Among all possible mothers Wavelet and thresholding settings combinations, select those that provide FHR distributions not statistically different from reference FHR distributions. Among the selected combinations, identify those characterized by the highest median SNR. Among the identified combinations, select as optimal the one that provides the lowest median ε_{FHR}.

Table 1. WT-based filters (F1 to F18) obtained by different combinations of three mothers Wavelet (4^{th}-order Coiflet, 4^{th}-order Daubechies and 8^{th}-order Symlet), two thresholding rules (Soft and Hard) and three thresholding algorithms (Universal, Rigorous and Minimax).

WT-based Filter	Mother Wavelet	Thresholding rule	Thresholding algorithm
F1	4^{th}-order Coiflet	Soft	Universal
F2	4^{th}-order Coiflet	Hard	Universal
F3	4^{th}-order Coiflet	Soft	Rigorous
F4	4^{th}-order Coiflet	Hard	Rigorous
F5	4^{th}-order Coiflet	Soft	Minimax
F6	4^{th}-order Coiflet	Hard	Minimax
F7	4^{th}-order Daubechies	Soft	Universal
F8	4^{th}-order Daubechies	Hard	Universal
F9	4^{th}-order Daubechies	Soft	Rigorous
F10	4^{th}-order Daubechies	Hard	Rigorous
F11	4^{th}-order Daubechies	Soft	Minimax
F12	4^{th}-order Daubechies	Hard	Minimax
F13	8^{th}-order Symlet	Soft	Universal
F14	8^{th}-order Symlet	Hard	Universal
F15	8^{th}-order Symlet	Soft	Rigorous
F16	8^{th}-order Symlet	Hard	Rigorous
F17	8^{th}-order Symlet	Soft	Minimax
F18	8^{th}-order Symlet	Hard	Minimax

3. Results

3.1. Simulated data

Results relative to the simulated FPCG data are reported in Table 2. Twelve filters (F1, F2, F3, F4, F5, F9, F11, F12, F13, F14, F15, F16) provided FHR not statistically different from the reference. Among them, those characterized by the highest median SNR (25.9 dB) were two, F1 and F13, with F1 being the one with the lowest median ε_{FHR} (1.3 bpm) with respect to reference. As a sample, Figure 3 depicts 10 s of simulated raw FPCG number 1 (SNR: 7.4 dB; in gray) and its filtered version (SNR: 14.4 dB; in black) obtained by application of F1 (4^{th}-order Coiflet; Soft thresholding rule; Universal thresholding algorithm).

Table 2. Values of FHR and SNR obtained at reference and after the application of the 18 WT-based filters (Table 1) to simulated and experimental FPCG data.
* and ** indicate $P < 0.05$ and $P < 0.01$, respectively, when comparing against reference.

		SIMULATED			EXPERIMENTAL		
		FHR (bpm)	**SNR (**dB)	ε_{FHR} (bpm)	**FHR (**bpm)	**SNR (**dB)	ε_{FHR} (bpm)
Reference		140.2 [139.7;140.7]	0.7 [−0.2;2.9]	-	140.5 [135.2;146.3]	15.6 [13.8;16.7]	-
WT-based filter	**F1**	138.7 [137.7;140.8]	25.9** [20.4;31.3]	1.3 [0.0;2.3]	139.6 [113.4;155.2]	22.9** [20.1;25.7]	0.9 [−14.6;28.7]
	F2	138.9 [137.9;140.8]	18.2** [15.8;22.7]	0.8 [0.0;2.2]	136.9** [111.8;146.2]	21.7** [18.8;25.2]	6.9 [−4.6;34.6]
	F3	140.3 [139.5;140.7]	14.3** [13.7;15.1]	0.1 [−0.4;0.6]	137.1 [109.8;149.7]	21.7** [18.8;25.2]	4.3 [−9.1;33.8]
	F4	140.1 [138.5;140.7]	11.4** [10.8;12.1]	0.2 [−0.1;1.3]	138.3* [113.1;147.9]	21.6** [18.6;24.9]	4.9 [−8.4;30.2]
	F5	138.8 [134.3;140.7]	21.9** [18.6;24.9]	1.2 [0.0;5.0]	132.9** [106.5;147.2]	22.8** [19.7;25.6]	7.4 [−8.1;34.8]
	F6	138.8* [135.1;140.7]	15.7** [14.1;16.9]	1.0 [0.0;4.1]	135.1** [111.1;146.9]	21.6** [18.7;25.1]	5.2 [−6.3;33.9]
	F7	139.2* [136.1;140.7]	26.3** [20.6;31.1]	1.0 [0.1;3.8]	139.1 [111.8;153.9]	22.9** [19.9;25.7]	1.7 [−14.2;28.9]
	F8	138.9** [135.8;140.7]	18.7** [16.1;23.5]	0.8 [0.0;4.1]	136.5** [110.8;145.2]	21.8** [18.8;25.2]	7.3 [−5.4;34.8]
	F9	140.3 [139.1;140.7]	14.5** [13.9;14.9]	0.1 [−0.2;0.9]	136.2* [109.8;149.9]	21.7** [18.8;25.2]	5.1 [−8.9;33.2]
	F10	139.3** [137.1;140.6]	11.6** [10.9;12.2]	0.7 [0.1;2.5]	138.3* [112.5;147.7]	21.6** [18.6;24.9]	5.0 [−8.2;30.5]
	F11	140.5 [136.1;140.7]	21.9** [18.6;24.9]	0.1 [−0.2;2.9]	133.1** [105.7;147.1]	22.8** [19.7;25.6]	8.0 [−7.5;34.5]
	F12	140.5 [136.5;140.7]	15.9** [14.5;17.3]	0.1 [0.0;2.4]	135.7** [109.6;145.5]	21.6** [18.7;25.2]	6.0 [−5.0;33.7]
	F13	138.6 [137.7;140.8]	25.9** [20.3;31.1]	1.6 [0.0;2.4]	139.4 [114.2;154.9]	22.9** [20.4;25.7]	1.3 [−15.4;27.7]
	F14	138.8 [137.6;140.8]	18.1** [15.8;22.3]	1.0 [−0.1;2.1]	134.3** [111.3;145.9]	21.7** [18.8;25.2]	8.2 [−5.0;34.6]
	F15	140.4 [139.5;140.7]	14.3** [13.9;15.1]	0.1 [−0.4;0.5]	136.4 [109.9;149.7]	21.7** [18.8;25.2]	4.0 [−9.3;33.2]
	F16	139.9 [138.5;140.6]	11.4** [11.1;12.1]	0.2 [0.0;1.4]	138.7* [111.9;147.8]	21.6** [18.6;24.9]	4.6 [−8.4;30.4]
	F17	138.6* [132.8;140.7]	21.8** [18.6;24.7]	1.2 [0.0;6.6]	133.1** [107.3;148.6]	22.8** [19.9;25.6]	7.0 [−8.5;35.2]
	F18	138.8* [133.9;140.7]	15.8** [14.5;17.1]	1.2 [0.0;5.6]	134.9** [109.8;146.5]	21.6** [18.7;25.1]	6.2 [−5.8;32.8]

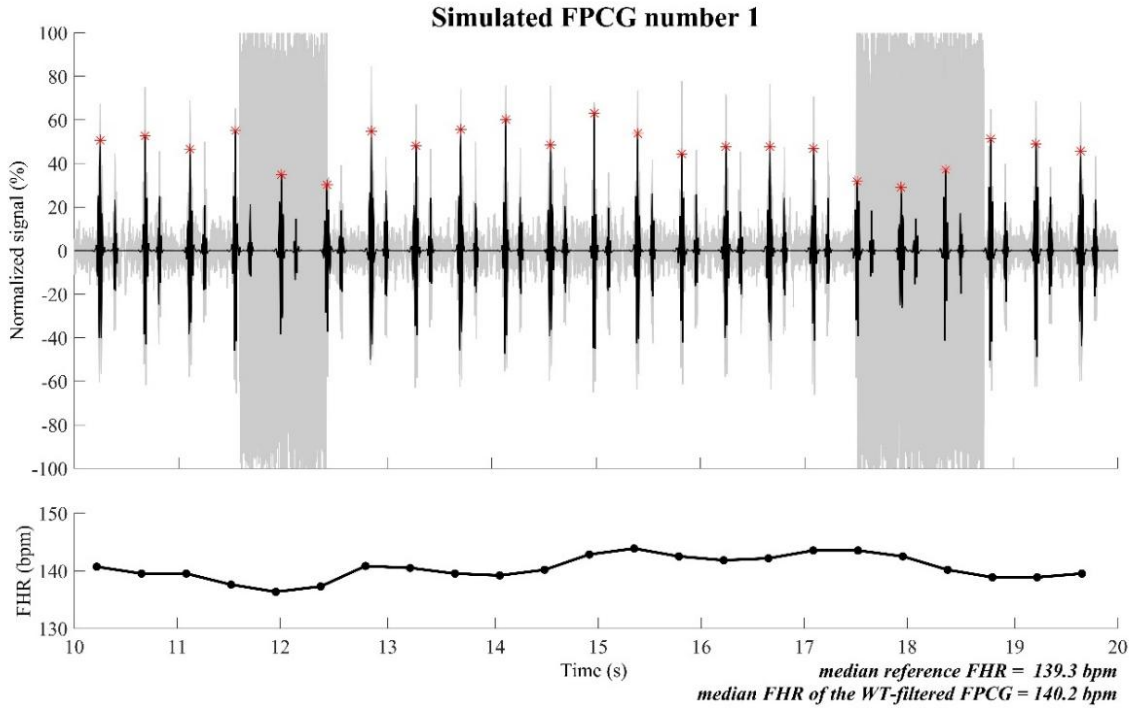

Figure 3. Upper panel: Graphical representation of 10 s of simulated raw FPCG number 1 (SNR: 7.4 dB; in gray), and its filtered version (SNR: 14.4 dB; in black) obtained by application of F1 (4^{th}-order Coiflet; Soft thresholding rule; Universal thresholding algorithm). Red stars indicate S1 sounds identification by PCG-Delineator [28]. Lower panel: Tachogram of the same 10s of simulated raw FPCG number 1. Beats are labeled with black spots.

3.2. Experimental data

Results relative to the experimental data are reported in Table 2. Five filters (F1, F3, F7, F13, F15) provided FHR not statistically different from the reference. Among them, those characterized by the highest median SNR (22.9 dB) were three, F1, F7 and F13, with F1 being the one with the lowest median ε_{FHR} (0.9 bpm) with respect to reference. As a sample, Figure 4 depicts 10 s of experimental raw FPCG number 5 (SNR: 15.5 dB; in gray), and its filtered version (SNR: 21.7 dB; in black) obtained by application of F1 (4^{th}-order Coiflet; Soft thresholding rule; Universal thresholding algorithm).

4. Conclusions

Any signal processing procedure finalized to remove noise from biomedical signals should be evaluated not only on noise features, such as mean square error and SNR, but also on clinical features. Indeed, it might happen that noise removal provides a very good-quality signal from which, however, some clinical features have been also deleted, making the filtered signal of limited clinical utility. WT-based filters have been proposed in literature as effective procedure to remove in-band noise from FPCG [2,11,12,21,24–30]. However, such filters have been mainly evaluated on noise

features [29,30]. Thus, the present work performed a comparative analysis of WT-based FPCG filtering approaches characterized by different combinations of mothers Wavelet and thresholding settings by considering both the SNR and the FHR. Only orthogonal mothers Wavelet (Coiflets, Daubechies, Symlets families) were found to be suitable to filter FPCG [26]; among them, the 4^{th}-order Coiflet is the most used one [21,26,29], often combined with 5 levels of decomposition [5,26,35] and Soft rule and Rigorous algorithm as thresholding settings [2,12,26,29,35]. No further investigation on the performance of the other possible combinations of mothers Wavelet and thresholding settings was so far been performed. Differently, the present work aimed to perform a comparative analysis of WT-based FPCG filtering approaches characterized by different combinations of mothers Wavelet and thresholding settings in order to identify the optimal WT-based filter for FPCG filtering. To this aim, three mothers Wavelet (the 4^{th}-order Coiflet, the 4^{th}-order Daubechies and the 8^{th}-order Symlet), two thresholding rules (Soft and Hard) and three thresholding algorithms (Universal, Rigorous and Minimax) were combined in all possible ways so that 18 different WT-based filters were obtained. Performance of these filters were then compared in order to identify the optimal one. Optimization was performed by minimizing loss of FPCG clinical information included in FHR and by maximizing noise reduction (i.e. by maximizing SNR). Evaluation was performed in both simulated and experimental FPCG data. In both cases, the WT-based filter obtained by combining the 4^{th}-order Coiflet mother Wavelet with the thresholding settings constituted by the Soft rule and the Universal algorithm (F1) resulted to be optimal one. By applying F1 to simulated FPCG, FHR was maintained (F1: 138.7[137.7; 140.8] bpm; Reference: 140.2[139.7; 140.7] bpm; $P > 0.05$; Table 2) while noise was strongly reduced (F1: SNR: 25.9[20.4; 31.3] dB; Reference SNR: 0.7[−0.2; 2.9] dB; $P < 10^{-14}$; Table 2). SNR values reported here were computed using Eq. 2 [21] and quantitatively differ from those reported in PhysioNet [4,31,32], possibly computed using a different formula; still the two SNR estimations are strongly linearly associated (correlation coefficient: 0.9996; $P < 10^{-57}$), thus carrying the same information. In this study, SNR values were recomputed in order to allow a comparative analysis after filtering. Similar results were obtained when applying F1 to experimental FPCG; FHR was maintained (F1: 139.6[113.4; 144.2] bpm; Reference: 140.5[135.2; 146.3] bpm; $P > 0.05$; Table 2) while SNR was strongly incremented (F1: 22.9[20.1; 25.7] dB; Reference: 15.6[13.8; 16.7] dB; $P < 10^{-37}$; Table 2).

Our optimal combination of mother Wavelet and thresholding settings (4^{th}-order Coiflet mother Wavelet, Soft thresholding rule, Universal thresholding algorithm) was slightly different from previously proposed as optimal (4^{th}-order Coiflet mother Wavelet, Soft thresholding rule, Rigorous thresholding algorithm) [29] mainly due to the introduction of clinical features in the evaluation criteria. Application of WT-based filters different from the optimal one on our data necessarily provided less satisfactory results. Nevertheless, it is interesting to highlight that, when using a specific mother Wavelet, Soft thresholding rule systematically provided better results than Hard thresholding rule. Moreover, there was no evidence about the existence of an optimal mother Wavelet when considered independently of associated thresholding settings. Rather, the performance of a WT-based filter strongly depends on the mother Wavelet-thresholding settings coupling [2,12,26,29,35], with the selection of thresholding settings being more relevant than the choice of mother Wavelet itself.

In conclusion, the WT-based filter obtained combining the 4^{th}-order Coiflet mother Wavelet with the thresholding settings constituted by the Soft thresholding rule and the Universal thresholding algorithm provides the optimal WT-based filter for FPCG filtering according to evaluation criteria based on both noise and clinical features.

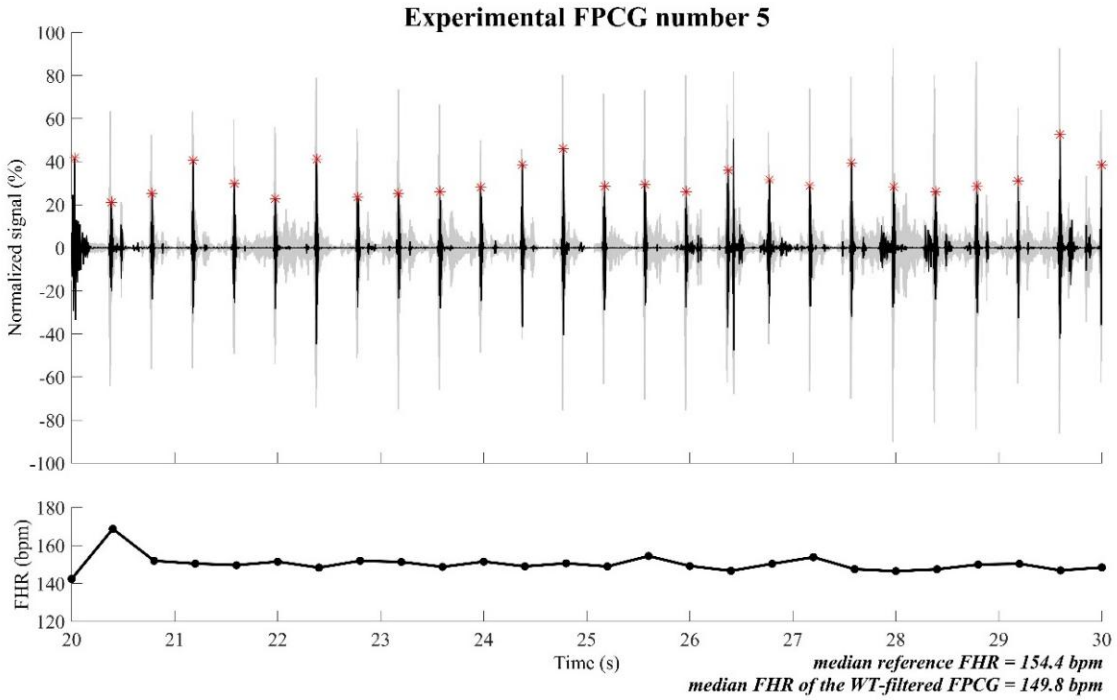

Figure 4. Upper panel: Graphical representation of 10 s of experimental raw FPCG number 5 (SNR: 15.5 dB; in gray) and its filtered version (SNR: 21.7 dB; in black) obtained by application of F1 (4^{th}-order Coiflet; Soft thresholding rule; Universal thresholding algorithm). Red stars indicate S1 sounds identification by PCG-Delineator [28]. Lower panel: Tachogram of the same 10 s of simulated raw FPCG number 1. Beats are labeled with black spots.

Acknowledgments

The authors wish to thank Prof. Reza Sameni for sharing the cardiotocographic data, simultaneously recorded to the fetal phonocardiographic data, without which reference values of the fetal heart rate in the experimental study could not be obtained.

Conflict of interest

All authors declare no conflicts of interest in this paper.

References

1. M. W. Trierweiler, R. K. Freeman and J. James, Baseline fetal heart rate characteristics as an indicator of fetal status during the antepartum period, *Am. J. Obstet. Gynecol.*, **125** (1976), 618–623.
2. V. S. Chourasia, A. K. Tiwari and R. Gangopadhyay, A novel approach for phonocardiographic signals processing to make possible fetal heart rate evaluations, *Digit. Signal Process.*, **30** (2014), 165–183.

3. I. Habermajer, F. Kovács and M. Török, A rule-based phonocardiographic method for long-term fetal heart rate monitoring, *IEEE Trans. Biomed. Eng.*, **47** (2000), 124–130.
4. M. Ruffo, M. Cesarelli, M. Romano, et al., An algorithm for FHR estimation from foetal phonocardiographic signals, *Biomed. Signal Process. Control*, **5** (2010), 131–141.
5. Y. Song, W. Xie, J. F. Chen, et al., Passive acoustic maternal abdominal fetal heart rate monitoring using wavelet transform, *Comput. Cardiol.*, **33** (2006), 581–584.
6. H. Tang, T. Li, T. Qiu, et al., Fetal heart rate monitoring from phonocardiograph signal using repetition frequency of heart sounds, *JECE*, (2016), 2404267.
7. J. Chen, K. Phua, Y. Song, et al., A portable phonocardiographic fetal heart rate monitor, *ISCAS*, (2006), 2141–2144.
8. J. P. Phelan and P. E. Lewis, Fetal heart rate decelerations during a nonstress test, *Obstet. Gynecol.*, **57** (1981), 228–232.
9. F. Kovács, C. Horváth, A. T. Balogh, et al., Fetal phonocardiography—past and future possibilities, *Comput. Methods Programs Biomed.*, **104** (2011), 19–25.
10. H. E. Bessil and J. H. Dripps, Real-time processing and analysis of fetal phonocardiographic sensor, *Clin. Phys. Physiol. Meas.*, **10** (1989), 67–74.
11. P. C. Adithya, R. Sankar, W. A. Moreno, et al., Trends in fetal monitoring through phonocardiography: challenges and future directions, *Biomed. Signal Process. Control*, **33** (2017), 289–305.
12. V. S. Chourasia and A. K. Tiwari, Design methodology of a new wavelet basis function for fetal phonocardiographic signals, *Sci. World J.*, (2013), Article ID 505840.
13. A. N. Pelech, The physiology of cardiac auscultation, *Pediatr. Clin. North. Am.*, **51** (2004), 1515–1535.
14. G. Anastasi, S. Capitani and M. Carnazza, in Trattato di anatomia umana, *Edi-Ermes*, **4** (2010), 321–324.
15. Z. Comert and A. F. Kocamaz, A study of artificial neural network training algorithms for classification of cardiotocography signals, *Bitlis Eren. Univ. J. Sci. Technol.*, **7**(2017), 93–103.
16. R. Sameni and G. Clifford, A review of fetal ECG signal processing; issues and promising directions, *Electrophysiol. Ther. J.*, **3** (2010), 4–20.
17. K. M. J. Verdurmen, C. Lempersz, R. Vullings, et al., Normal ranges for fetal electrocardiogram values for the healthy fetus of 18–24 weeks of gestation: A prospective cohort study, *BMC Pregnancy Childbirth*, **16** (2016), 227.
18. A. Agostinelli, M. Grillo, A. Biagini, et al., Noninvasive fetal electrocardiography: An overview of the signal electrophysiological meaning, recording procedures, and processing techniques, *Ann. Noninvasive Electrocardiol.*, **20** (2015), 303–313.
19. M. Sato, Y. Kimura, S. Chida, et al., A novel extraction method of fetal electrocardiogram from the composite abdominal signal, *IEEE Trans. Biomed. Eng.*, **54** (2007), 49–58.
20. V. S. Chourasia and A. K. Tiwari, A review and comparative analysis of recent advancements in fetal monitoring techniques, *Crit. Rev. Biomed. Eng.*, **36** (2008), 335–373.
21. A. Sbrollini, A. Strazza, M. Caragiuli, et al., Fetal phonocardiogram denoising by wavelet transformation: robustness to noise, *Comput. Cardiol.*, **44** (2017), 1–4.
22. M. Samieinasab and R. Sameni, Fetal phonocardiogram extraction using single channel blind source separation, *ICEE 2015*, (2015), 78–83.

23. A. Khandoker, E. Ibrahim, S. Oshio, et al., Validation of beat by beat fetal heart signals acquired from four-channel fetal phonocardiogram with fetal electrocardiogram in healthy late pregnancy, *Sci. Rep.*, **8** (2018), 13635.
24. A. Jimenez, M. R. Ortiz, M. A. Pena, et al., The use of wavelet packets to improve the detection of cardiac sounds from the fetal phonocardiogram, *Comput. Cardiol.*, **26** (1999), 463–466.
25. E. Koutsiana, L. J. Hadjileontiadis, I. Chouvarda, et al., Detecting fetal heart sounds by means of fractal dimension analysis in the wavelet domain, *EMBC 2017*, (2017), 2201–2204.
26. D. Messer, S. Agzarian and J. Abbott, Optimal wavelet denoising for phonocardiograms, *Microelectron. J.*, **32** (2001), 931–941.
27. S. Vaisman, S.Y. Salem and G. Holcberg, Passive fetal monitoring by adaptive wavelet denoising method, *Comput. Biol. Med.*, **42** (2012), 171–179.
28. A. Strazza, A. Sbrollini, V. Di Battista, et al., PCG-Delineator: an efficient algorithm for automatic heart sounds detection in fetal phonocardiography, *Comput. Cardiol.*, **45** (2018), 1–4.
29. V. S. Chourasia and A. K. Mittra, Selection of mother wavelet and denoising algorithm for analysis of foetal phonocardiographic signals, *J. Med. Eng. Technol.*, **33** (2009), 442–448.
30. V. S. Chourasia and A. K. Mittra, Most suitable mother wavelet for fetal phonocardiographic signal analysis, *IJFET*, **4** (2009), 23–29.
31. A. L. Goldberger, L. A. Amaral, L. Glass, et al., PhysioBank, PhysioToolkit, and PhysioNet: components of a new research resource for complex physiologic signals, *Circulation*, **101** (2000), 215–220.
32. M. Cesarelli, M. Ruffo, M. Romano, et al., Simulation of foetal phonocardiographic recordings for testing of FHR extraction algorithms, *Comput. Methods. Programs Biomed.*, **107** (2012), 513–523.
33. C. Liu, D. Springer, Q. Li, et al., An open access database for the evaluation of heart sound algorithms, *Physiol. Meas.*, **37** (2016), 2181–2213.
34. A. Misal, G. R. Sinha, R. M. Potdar, et al., Comparison of wavelet transforms for denoising and analysis of PCG signal, *JCS*, **1** (2012), 1–5.
35. B. Ergen, Comparison of wavelet types and thresholding methods on wavelet based denoising of heart sounds, *JSIP*, **4** (2013), 164–167.

AIMS Press